Anatomic and functional mapping of human uterine innervation

Marion Pinsard, Nicolas Mouchet, Ludivine Dion, Thomas Bessede, Martin Bertrand, Emile Darai, Pascale Bellaud, Philippe Loget, Séverine Mazaud-Guittot, Xavier Morandi, et al.

Running title: Analysis of uterine micro-innervation

Anatomical and functional mapping of uterine innervation in the human

Marion PINSARD, MD[1], Nicolas MOUCHET, PhD[2], Ludivine DION, MD[1], Thomas BESSEDE, MD, PhD[3,4], Martin BERTRAND, MD, PhD[5], Emile DARAI, MD, PhD[6], Pascale BELLAUD[7], Philippe LOGET, MD[8], Séverine MAZAUD-GUITTOT, MD, PhD[9], Xavier MORANDI, MD, PhD[10,11], Jean LEVEQUE, MD, PhD[1], Vincent LAVOUÉ, MD, PhD[1,12], Martha DURAES, MD[5], Krystel NYANGOH TIMOH, MD, PhD[1,9,12,13].

Affiliations:

[1] Department of Obstetrics and Gynecology, Hopital Universitaire de Rennes, university Rennes 1, Rennes, France.

[2] University Rennes 1, CNRS, Inserm UMS Biosit, France BioImaging, Core Facility H2P2 Rennes, F-35000, France

[3] UMR 1195, University Paris Sud, INSERM, Université Paris-Saclay, 94270, Le Kremlin-Bicetre, France

[4] Urology Department, Hopitaux Universitaires Paris-Sud, APHP, 94270, Le Kremlin-Bicetre, France

[5] Centre Hospitalier Universitaire de Nîmes, Nîmes.

[6]Service de gynécologie obstétrique et médecine de la reproduction, Hôpital Tenon, AP-HP, Sorbonne Université, 4 rue de la Chine, Paris 75020, France ; INSERM UMRS 938, Centre de Recherche Saint-Antoine, 27 rue Chaligny, PARIS cedex 12 75571, France.

[7]Université de Rennes 1, Rennes, France ; INSERM, UMR991 Liver Metabolism and Cancer, Rennes, France.

[8] Service d'Anatomie et Cytologie Pathologiques, CHU Rennes, Rennes, France.

[9] Inserm, EHESP, Irset (Institut de Recherche en Santé, Environnement et Travail) UMR_S 1085, University Rennes, 35000, Rennes, France

[10] Laboratoire d'Anatomie et d'Organogenèse, Faculté de Médecine, Centre Hospitalier Universitaire de Rennes, 2 Avenue du Professeur Léon Bernard, 35043 Rennes Cedex, France.

[11] Department of Neurosurgery, Rennes University Hospital, Rennes, France.

[12] Department of Obstetrics and Gynecology, CHU Rennes Hospital, 35000, and SAFE CIC 1414 Thematic Team, CHU Rennes, Rennes, France.

[13] Department of Obstetrics and Gynecology, Rennes Hospital, France; Rennes, University 1, Rennes, France, INSERM, LTSI - UMR 1099, France.

Corresponding author:
Krystel NYANGOH TIMOH, MD, PHD
Department of Obstetrics and Gynecology,
Hôpital Sud, 16, Boulevard de Bulgarie,
Rennes, 35200, France
Tel : +33 06 72 13 60 50
krystel.NYANGOH.TIMOH@chu-rennes.fr

Capsule:

We provide a three-dimensional reconstruction model of the autonomic sympathetic, parasympathetic and sensitive nerves of the uterus.

STRUCTURED ABSTRACT

Objective: To better understand the physiology of pain in pelvic pain pathologies such as endometriosis, in which alterations of uterine innervation have been highlighted, we carried out an anatomical and functional mapping of the macro- and micro-innervation of the human uterus. Our aim was to provide a three-dimensional reconstruction model of uterine innervation.

Design: This was an experimental study. We dissected the pelvises of four human female fetuses into serial sections, and treated them with HES before immunostaining.

Setting: Academic Research Unit

Patients: None

Interventions: None

Main outcome measures: Detection of nerves (S100 +) and characterization of the types of nerves. The slices obtained were aligned to construct a three-dimensional model.

Results: A three-dimensional model of uterine innervation was constructed. The nerve fibers appeared to have a centripetal path from the uterine serosa to the endometrium. Within the myometrium, innervation was dense. Endometrial innervation was sparse but present in the functional layer of the endometrium. Overall innervation was richest in the supra-vaginal cervix and rarer in the body of the uterus. Innervation was rich particularly laterally to the cervix next to the parametrium and the paracervix. Four types of nerve fibers were identified: autonomic sympathetic (TH+), parasympathetic (VIP+), and sensitive (NPY+, CGRP1+ and VIP+). They were found in the three portions and the three layers of the uterus.

Conclusions: We constructed a three-dimensional model of the human uterine innervation. This model could provide a solid base for studying uterine innervation in pathological situations, in the hope of finding new therapeutic approaches.

Key words: neuro-anatomy – uterine innervation – endometriosis - benign pelvic disease - chronic pelvic pain

INTRODUCTION

Complex benign pelvic diseases ─such as chronic pelvic pain, endometriosis, myomas and adenomyosis─ are frequent and can considerably affect a women quality of life(1). Many studies suggest that they are associated with uterine and pelvic innervation abnormalities(2–9). Tokushigue et al demonstrated that patients with endometriosis have an autonomic innervation of the superficial layer of the endometrium unlike control patients(7). However, in a cohort of patients with myomas or adenomyosis, Zhang et al showed that only patients with pain-had innervation of the functional layer as well as significantly higher innervation of the myometrium(9). Moreover, Ellet et al demonstrated that nerve fibers were present in the endometrium of patients with and without endometriosis in a cohort of patients with pain (10). Furthermore, Quinn et al described micro-neuromas within the myometrium in patients with chronic pelvic pain(5). These results suggest that uterine innervation is involved in complex benign pelvic diseases, and particularly in nociceptive mechanisms associated with pelvic pain.

However, few data have been published about the organization and specificity of intra-uterine innervation in the human and its relation to uterine portions and layers. New anatomical techniques such as immunohistochemistry, fluorochromes and computer-assisted anatomical dissection (CAAD) have been developed to study pelvic neuro-anatomy in recent years, with clinical and surgical implications(11–13).

Our aim was to study the functional anatomy of uterine micro-innervation with a CAAD technique and to provide a comprehensive three-dimensional (3D) reconstruction to develop a clinical correlation for the practicing physician.

MATERIAL AND METHODS

Human fetuses

The fetal specimens were obtained from late miscarriages which were not secondary to chorioamnionitis or known genetic abnormalities, and without genito-urinary malformation. All parents gave written consent for the scientific use of the cadaver. Only specimens without maceration, or morphological or macroscopic neurological abnormalities on pathology examination were used. The French Biomedicine Agency approved the study (PFS09-011). The work was compliant with the provisions of the 2013 revised version of the Declaration of Helsinki. Four female fetuses, aged at 21, 24, 26, and 27 weeks of gestation, as determined from the crown-rump length(14), were studied. The external body aspect of each fetus was carefully restored after the autopsy.

Histological conditioning

The entire pelvis was removed en-bloc with the pelvic organ and pelvic bone, and was fixed in formalin (4% formaldehyde) for 6 days. Tissues were then cut into transverse or sagittal slices at 4-mm intervals. The tissue slices were placed in baskets, processed, and embedded in cardboard molds filled with paraffin. To avoid alteration of the visceral topographical relationship, the slices were kept warm in water at 37°C and then mounted whole on Superfrost glass slides. They were then dried at 56°C overnight. We obtained a total of 1000 to 2000 sections from each fetus, depending on the age and size of the specimen.

Staining and immunolabeling

The first section of each level was taken as the reference and was stained with Hematoxylin Eosin Safran (HES) to determine the main anatomical structures (collagen tissue in yellow, cytoplasm in pink, nuclei in purple).

Smooth muscles were detected with polyclonal antibodies against α-smooth muscle actin (SMA)(15). Neuronal markers were detected with polyclonal antibodies against protein S100 (PS100) for the labeling all nerves(16), peripheral myelin protein (PMP 22) for the somatic peripheral nerves(17), tyrosine hydroxylase (TH) for sympathetic nerves(18), vesicular acetylcholine transferase (VAChT) for parasympathetic neurons(19), the neural isoform of nitric oxide synthase (nNOS) for the pro-erectile nerve bundles(20), vaso-intestinal peptide (VIP) for parasympathetic and sensitive nerve fibers(21), neuropeptide Y (NPY) for sympathetic and sensitive nerve fibers(21), calcitonin gene-related peptide (CGRP) for sensitive fibers(22), and oxytocin and relaxin-2 (RLN2) for nerves involved in contraction and relaxation of smooth muscle(23) (Table 1).

All immunostaining was automated (DISCOVERY Ultra system from Roche ®, Illkirch, France).The different steps were as follows: 1) Dewaxing (72°C) and rehydration (Discovery Wash - Ref: 07311079001-Roche); 2) Antigenic unmasking (citrate pH 6 or EDTA pH 8 at 95°C); 3) Inactivation of endogenous peroxidase with hydrogen peroxide; 4) Application and incubation of the primary antibody at the right dilution (Supplemental Table 1); 5) Incubation of the secondary antibody (OmniMap anti-MsHRP, ref 0526965001-Roche, or OmniMap anti-RbHRP, ref 05269679001-Roche), coupled with an enzyme, the horseradish peroxidase (HRP); 6) Revelation (ChromoMap DAB, ref 05269652001-Roche) and 7) Counter-staining (Hematoxylin II, ref 05277965001-Roche).

Immunofluorescence

Co-staining was obtained by means of a fluorescent multiplex technique using fluorophore-conjugated tyramide. Three kinds of fluorophores were used: rhodamine (ref 07259883001-Roche), Cyanine 5 (ref 07551215001-Roche) and FAM (ref 07988150001-Roche), and DAPI ((4',6-diamidino-2-phénylindole, ref 0526688001-Roche) which colors the nuclei.

Image analysis

Two-dimensional (2D) serial stained and immunolabeled sections were used for the 3D reconstruction. Using high magnification (4× to 40×) analyses of the HES-stained sections, it was possible to identify the various anatomical structures (organs, bones, and fascia). Subsequent sections, treated with an antibody against S100, were used to identify pelvic nerves and communicating branches. We compared the HES-stained sections with sections stained with specific antibodies against SMA and S100 firstly, and then with the other antibodies. In this way it was possible to study the path of the nerve fibers towards the uterus, and within its different parts and layers, and to determine the specificity of these nerves.

The computer system comprised a personal laptop computer (Windows XP) equipped with an Epson Perfection V750 digitization system, Silverfast AI digitization software (Ref B11B178071), Adobe Photoshop image-processing software, and Surfdriver software for Windows (Winsurf image reconstruction software, version 4.3). All sections were digitized at a resolution of 4800 dots per inch, and the images were then stacked and aligned. The brightness and contrast of the histological tissue images were adjusted using Adobe Photoshop. The pelvic anatomical structures and nerve fibers were outlined manually on all histological sections.

We also used HALO® software (version 3.0.311.255) to perform objective automated nerve quantification on the immunofluorescence slices (Figure 1) in three portions of the uterus (supra-vaginal cervix, intra-vaginal cervix, and uterine body), and in four uterine layers:

peritoneal serosa, myometrium, the basal endometrial layer (deep layer adjacent to the myometrium which undergoes little menstrual change and is not expelled at the end of cycle), and the functional layer (containing the thick intermediate (spongy) layer, and the top thinner (compact) layer, undergoing significant menstrual changes and expelled at the end of cycle). The density of the nerve fibers was calculated as a percentage of the studied surface area.

Finally, a 3D analysis of the location, course, and distribution of the nerve fibers was carried out and an animated reconstruction generated (Supplemental Figure/video 1).

RESULTS

Uterine innervation in the human fetal models

Two-dimensional observations

The entry point of the uterine nerve fibers is lateral to the uterine isthmus and cervix. Nerve fibers arise directly from the inferior hypogastric plexus.

Organization of uterine innervation

Uterine innervation is centripetal and runs from the uterine serosa to the endometrium (Figure 1). The uterine nerves penetrate the myometrium and become less dense as they reach the endometrium.

Myometrial innervation is dense (Figure 1) and preferentially perivascular, but also sometimes peri-muscular (Figure 2). Uterine innervation formed a linear organization within the myometrium.

Endometrial innervation does exist but is sparse. We observed nerves within all the layers of the endometrium with a linear organization within the functional layer of the endometrium. (Supplemental Figure 2 and Supplemental Figure 3).

Density of nerves in the uterus (Supplemental Figure 4)

Nerve density varies widely between the different portions of the uterus: denser at the cervix and less dense in the uterine body. Nerves penetrate the uterus at the uterine isthmus with most of them then clustering around the cervix and others running up and down.

Nerve density also varies between the different uterine layers as previously described according to the centripetal disposition of uterine innervation. It is denser at the periphery within the serosa particularly laterally to the cervix next to the parametrium and paracervix.

Specificity / function of uterine innervation (Table 1)

We found four types of nerve labeling in the uterus: sympathetic (TH+ and NPY+), parasympathetic (VIP+), and sensitive nerve fibers (NPY+, CGRP1+ and VIP+). They are found in all portions and layers of the uterus (Supplemental Figure 5, Supplemental Figure 6, Supplemental Figure 7, Supplemental Figure 8).

The dominant nerve fibers are sympathetic (TH+). The second dominant nerve fibers are sympathetic and sensitive (NPY+). The third dominant nerve fibers are sensitive (CGRP1+) and the last are parasympathetic and sensitive (VIP+).

The preferential portions for these specific nerves are the cervix (TH+ with 79% of fibers, NPY+ with 73% of fibers and VIP+ 13%) and the uterine body for CGRP1+fibers (63% of nerves).

The preferential layers are the level of the serosa of the supra-vaginal cervix, i.e., in contact with the paracervix for TH+ fibers and the myometrium for NPY+ and CGRP+ fibers.

TH+, NPY+, CGRP+ and VIP+ nerve fibers are present in the functional layer of the endometrium. NPY+ and CGRP+ fibers are the most common, and VIP+ the least; NPY+ and CGRP1+ sensitive and TH+ sympathetic nerve fibers penetrate the functional layer.

There are no parasympathetic (VAChT+), nitrergic (nNOS+), or somatic (PMP22+) nerve fibers, nor oxytocin+ or RLN2+ fibers.

Innervation of the fetal uterine artery

Innervation of the uterine artery is rich (Supplemental Figure 9). Autonomous innervation of the artery mainly consisted of sympathetic fibers (TH+). Parasympathetic (VAChT+), nitrergic (nNOS+), and sensitive (NPY+, CGRP1+) nerve fibers are also observed.

Three-dimensional reconstruction of fetal uterine innervation

We reconstructed a 3D uterine micro-innervation model focusing on the lower part of the uterus (Figure 3). Nerve fibers penetrate the uterus through the lateral edges of the uterine isthmus. They then follow a centripetal path from the periphery (serosa) to the center (endometrium) with ascending fibers towards the uterine body and descending fibers towards the cervix (Supplemental Figure/video 1).

DISCUSSION

We present here the first description of the distribution of specific nerves throughout the human uterus accompanied by a comprehensive 3D reconstruction of uterine innervation based on a fetal model. The principal results of this study are that 1) fetal uterine innervation is essentially composed of sympathetic and parasympathetic fibers, and sensitive nerves, 2) all the layers of the uterus are innervated with a centripetal disposition including the endometrium, and 3) nerve fibers penetrate the uterus through the lateral edges of the isthmus.

Mature human fetuses are considered valid and reliable experimental models for pelvic neuroanatomic studies(24,25). Human fetal tissue has previously been used for pelvic innervation and muscle studies as pelvic innervation is fully developed at 8 weeks of gestation. This was reported in a fetus study by Fritsch(25), and later observed by Arango-Toro(24) in an anatomical study of 15 human embryos and two fetuses ranging in size from 4 to 132 mm crown-rump length: the pelvic plexus was fully developed by Carnegie stage 23. Consequently, pelvic neuroanatomy is stable and comparable with that of the adult after 8 weeks of gestation with no further fundamental changes occurring during fetal growth and post-fetal development. There are several advantages to using fetal tissue. First, the small size of the fetus enables en-bloc pelvis removal and processing, minimizing anatomical data loss, surgical displacement and reconstruction biases compared to adult specimens and surgical dissection. Second, we performed continuous serial sections and were thus able to follow the nerve pathways. Third, nerves are larger in fetuses than in adults proportionally. Finally, multiple specific muscular and neuronal markers can be used in fresh material.

We used a technique called computer assisted anatomical dissection (CAAD) which was introduced in the 90’s by Benoit’s team(26). This original technique provides an accurate 3D reconstruction of fetal anatomy with identification of the exact organization of the thin nerve elements, their distribution, and their relationship to the vascular, visceral, fascial and muscular structures(27). CAAD is now used by various teams around the world (28–30). In this study, we further improved the basic technique by the addition of co-labelling and immuno-fluorescence. This allowed us to identify several types of nerves as well as uterine smooth muscle in the same image so as to clearly distinguish myometrial from endometrial innervation. Additionally, fluorochromes provided a high discrimination of markings for nerve quantification, which is more objective and compatible with the use of automated nerve quantification software.

Few data exist about the micro-innervation of the human uterus as most studies to date have been conducted on animal models(22,31,32). In the present study, we observed that innervation of the myometrium is dense, and that the nerves follow blood vessels or smooth muscle cells. These findings are in agreement with the literature(31). In 1959, Krantz et al employed the term "nerve plexus" to describe nerves within the human myometrium, based on works dating from the 18 century(33). The presence of endometrial innervation is a matter of debate. In this study, we observed that uterine innervation reached the superficial layer of the endometrium. In most mammalian species, the endometrium has been described as being poorly innervated(22,31,32). In the human uterus, Coupland(34), Krantz, Quinn(5,33) and other authors failed to identify nerves within the basal and superficial endometrium except in pathologic conditions(6,9,10,35).

Few studies have described the specificity of the nerves within the uterus in physiologic conditions. In our study, we observed that uterine innervation was composed exclusively of autonomic nerve fibers. We chose to use specific neurotransmitters to label uterine innervation function as in previous studies: TH+, NPY+ for autonomic sympathetic fibers, and VIP+, NOS+ and VACHT+ for autonomic parasympathetic fibers. Also, as demonstrated by Tokushigue et al, CGRP1+, VIP+ and NPY+ could also be markers for sensitive A delta- and C-type nerve fibers. We found a dense proportion of sympathetic (TH+, NPY+) and parasympathetic (VIP+) fibers in the cervix, and a high proportion of sensitive (CGRP1+) nerves in the uterine body. These results are in concordance with the study by Coupland and Di Tommaso showing that parasympathetic nerve fibers are mainly localized in the cervix(23)·(34). We also found that the functional layer of the endometrium is already innervated in the female fetus with highly sympathetic (TH+, NPY+) and sensitive (CGRP and NPY+) nerves. Recent studies showing nerves within the endometrium or myometrium in the human uterus in pathologic conditions only identified autonomic sensitive, sympathetic and parasympathetic nerves(6,9,10,35). This discrepancy with previous studies is related to our specimens of prepubescent uteri. Furthermore, one could speculate that the superficial layer of the endometrium is denervated during puberty secondary to exposure to estrogen(36). We thus suggest that the lack of denervation of the functional endometrium during puberty is a possible nociceptive mechanism.

The function of individual neurotransmitters is poorly understood to date. Sympathetic (TH+, NPY+) nerve fibers may be responsible for endometrial glandular secretion and vasoconstriction. Parasympathetic (VIP+, VACHT+, NOS+) and CGRP1+ are more likely involved in vasodilatation and uterine relaxation.

From a physiologic point of view, dense autonomic uterine innervation is fundamental for uterine function. Unsurprisingly, we observed that uterine innervation was composed exclusively of autonomic nerve fibers with a peri-vascular and peri-muscular organization. This could explain how uterine innervation is involved in contractile activity allowing uterine cyclic peristalsis and uterine contractions during labor. The dense innervation of the cervix that we describe here is coherent with the important role of cervical ripening during labor and menstruation(36). Dysregulation of uterine innervation could affect fertility by disrupting uterine muscle peristalsis and impairing blood flow regulation(35).

From a clinical point of view, gynecologic pathologic conditions are associated with uterine innervation abnormalities. Endometriotic lesions infiltrate richly innervated anatomic sites, contain abnormal innervation, and develop along the nerves(2,8). Additionally, patients with endometriosis, myomas, or adenomyosis who suffer from pain display innervation of the functional layer of endometrium and a significantly higher innervation of the myometrium than patients without pain(7),[9,10]. Atwal et al also showed that pelvic pain was associated with abnormal reinnervation and micro-neuromas within the myometrium(37). Finally, Ellet et al demonstrated that nerve fibers were present in the endometrium of patients with and without endometriosis in a cohort of patients with pain (10). These results suggest the involvement of endometrial innervation in pain mechanisms rather than in a specific gynecologic disease such as endometriosis. In these pathologic conditions associated with greater innervation density, the role of neurotransmitters can be altered. TH+ and NPY+ enable angiogenic and neurotrophic factors that increase blood vessels and nerve density. VIP+ and CGRP1+ contribute to the inflammatory response. CGRP1+, VIP+ and NPY+ present in sensitive C and A delta fibers may convey information to the central nervous system about the internal environment and potential noxious stimuli (Table 1).

Despite these results and the use of an original model, our study has some limitations. First, the use of a fetal model with an immature prepubescent uterus is possibly debatable: hormonal changes during puberty could explain some of the surprising results such as the lack of oxytocin or nNos labeling. According to Bauer et al, there is marked diminution of nerve density at puberty. Additionally, cyclic variations in the levels of sex hormones influence uterine innervation, especially sympathetic nerve fibers(36). Sympathetic nerve fibers express estrogen receptors which suggests that estrogen may regulate their plasticity. In animal models, increased estrogen levels during the cycle precede the disappearance of

uterine sympathetic nerves. During pregnancy, there is also a loss of sympathetic, parasympathetic and afferent nerves secondary to sexual hormone expression (estrogen and progesterone), mechanical strain, hypertrophy of the myometrium and local influence of the placenta(36).

There is thus a need for comparative studies of fetal and adult pelvic neuroanatomy. At our center in Rennes, we plan to investigate uteruses from brain-dead donors during multiple organ procurement in the context of a study about uterus transplantation. However, this is the first study to provide a comprehensive model of uterine innervation. Second, the small sample size cannot exclude biases. Nevertheless, the same pattern of uterine innervation was observed in all four fetuses. Moreover, we analyzed the whole uterus avoiding the bias of the variability of innervation of the endometrium. Third, functional relevance is not necessarily associated with clinical relevance. However, the use of neuronal antibodies contributed to the understanding of innervation pathways. Finally, the absence of a somatic uterine innervation may be related to the fact that myelinization is a late event during fetal development. However, using smooth muscle immunostaining, we observed that the whole uterus was smooth and so exclusive autonomic innervation was coherent.

CONCLUSION

We provide here the first comprehensive description of the innervation of the human uterus. This could serve as a basis for future studies on changes in uterine innervation caused by normal physiologic or pathophysiologic conditions.

Acknowledgements:

The authors want to express their gratitude to the parents who consented to donate a fetal body to science after late miscarriage.

The authors want also to acknowledge Jean-Eric Berton and Julien Landreau for the technical support.

References

1. Pynnä K, Räsänen P, Sintonen H, Roine RP, Vuorela P. The health-related quality of life of patients with a benign gynecological condition: a 2-year follow-up. J Comp Eff Res 2021;10:685–95.

2. Anaf V, Simon P, El Nakadi I, Fayt I, Simonart T, Buxant F, et al. Hyperalgesia, nerve infiltration and nerve growth factor expression in deep adenomyotic nodules, peritoneal and ovarian endometriosis. Hum Reprod 2002;17:1895–900.

3. Quinn MJ. Endometriosis: the consequence of uterine denervation-reinnervation. Arch Gynecol Obstet 2011;284:1423–9.

4. Quinn M. Uterine innervation in fibroids: a qualitative study. J Obstet Gynaecol 2007;27:489–92.

5. Quinn MJ, Kirk N. Differences in uterine innervation at hysterectomy. American Journal of Obstetrics and Gynecology 2002;187:1515–20.

6. Tokushige N, Markham R, Russell P, Fraser IS. Different types of small nerve fibers in eutopic endometrium and myometrium in women with endometriosis. Fertility and Sterility 2007;88:795–803.

7. Tokushige N, Markham R, Russell P, Fraser IS. High density of small nerve fibres in the functional layer of the endometrium in women with endometriosis. Hum Reprod 2006;21:782–7.

8. Tokushige N, Markham R, Russell P, Fraser IS. Nerve fibres in peritoneal endometriosis. Hum Reprod 2006;21:3001–7.

9. Zhang X, Lu B, Huang X, Xu H, Zhou C, Lin J. Innervation of endometrium and myometrium in women with painful adenomyosis and uterine fibroids. Fertility and Sterility 2010;94:730–7.

10. Ellett L, Readman E, Newman M, McIlwaine K, Villegas R, Jagasia N, et al. Are endometrial nerve fibres unique to endometriosis? A prospective case–control study of endometrial biopsy as a diagnostic test for endometriosis in women with pelvic pain. 2015 Dec;30:2808-15.

11. Nyangoh Timoh K, Bessede T, Lebacle C, Zaitouna M, Martinovic J, Diallo D, et al. Levator ani muscle innervation: Anatomical study in human fetus. Neurourol Urodyn 2017;36:1464–71.

12. Nyangoh Timoh K, Moszkowicz D, Zaitouna M, Lebacle C, Martinovic J, Diallo D, et al. Detailed muscular structure and neural control anatomy of the levator ani muscle: a study based on female human fetuses. American Journal of Obstetrics and Gynecology 2018;218:121.e1-121.e12.

13. Alsaid B, Karam I, Bessede T, Abdlsamad I, Uhl J-F, Delmas V, et al. Tridimensional computer-assisted anatomic dissection of posterolateral prostatic neurovascular bundles. Eur Urol 2010;58:281–7.

14. Hern WM. Correlation of fetal age and measurements between 10 and 26 weeks of gestation. Obstet Gynecol 1984;63:26–32.

15. Kobayashi M, Inoue K, Warabi E, Minami T, Kodama T. A Simple Method of Isolating Mouse Aortic Endothelial Cells. Journal of Atherosclerosis and Thrombosis 2005;12:138–42.

16. Hollabaugh RS, Dmochowski RR, Steiner MS. Neuroanatomy of the male rhabdosphincter. Urology 1997;49:426–34.

17. Bremer J, Baumann F, Tiberi C, Wessig C, Fischer H, Schwarz P, et al. Axonal prion protein is required for peripheral myelin maintenance. Nature Neuroscience 2010;13:310–8.

18. Butler-Manuel SA. Pelvic Nerve Plexus Trauma at Radical and Simple Hysterectomy: A Quantitative Study of Nerve Types in the Uterine Supporting Ligaments. 2002;9:47-56

19. Usdin T, Eiden L. Molecular biology of the vesicular transporter. 1995;18:218-24

20. Moszkowicz D, Alsaid B, Bessede T, Zaitouna M, Penna C, Benoit G, et al. Neural Supply to the Clitoris: Immunohistochemical Study with Three-Dimensional Reconstruction of Cavernous Nerve, Spongious Nerve, and Dorsal Clitoris Nerve in Human Fetus. The Journal of Sexual Medicine 2011;8:1112–22.

21. Cohen DP, Ikeda SR, Lewis DL. Neuropeptide Y and Calcitonin Gene-Related Peptide Modulate Voltage-Gated Ca2+ Channels in Mature Female Rat Paracervical Ganglion Neurons. J Soc Gynecol Investig. 1996;3:342-9.

22. Gnanamanickam GJE, Llewellyn-Smith IJ. Innervation of the rat uterus at estrus: a study in full-thickness, immunoperoxidase-stained whole-mount preparations. J Comp Neurol 2011;519:621–43.

23. Di Tommaso S, Cavallotti C, Malvasi A, Vergara D, Rizzello A, De Nuccio F, et al. A Qualitative and Quantitative Study of the Innervation of the Human Non Pregnant Uterus. Curr Protein Pept Sci 2017;18:140–8.

24. Arango-Toro O, Domenech-Mateu JM. Development of the pelvic plexus in human embryos and fetuses and its relationship with the pelvic viscera. Eur J Morphol 1993;31:193–208.

25. Fritsch H. Topography of the pelvic autonomic nerves in human fetuses between 21?29 weeks of gestation. Anatomy and Embryology 1989;180:57–64.

26. Benoit G, Quillard J, Ledroux X, Caillaux F, Bensadoun H, Jardin A. [Computer-assisted prostate reconstruction]. Ann Urol (Paris) 1990;24:585–7.

27. Alsaid B, Bessede T, Diallo D, Karam I, Uhl JF, Delmas V, et al. Computer-assisted anatomic dissection (CAAD): evolution, methodology and application in intra-pelvic innervation study. Surg Radiol Anat 2012;34:721–9.

28. Wallner C, Dabhoiwala NF, DeRuiter MC, Lamers WH. The anatomical components of urinary continence. Eur Urol 2009;55:932–43.

29. Bardol T, Subsol G, Perez M-J, Genevieve D, Lamouroux A, Antoine B, et al. Three-dimensional computer-assisted dissection of pancreatic lymphatic anatomy on human fetuses: a step toward automatic image alignment. Surg Radiol Anat 2018;40:587–97.

30. Balaya V, Guimiot F, Bruzzi M, El Batti S, Guedon A, Lhuaire M, et al. Feasibility of a fetal anatomy 3D atlas by computer-assisted anatomic dissection. J Gynecol Obstet Hum Reprod 2020;49:101880.

31. Adham N, Schenk EA. Autonomic innervation of the rat vagina, cervix, and uterus and its cyclic variation. American Journal of Obstetrics and Gynecology 1969;104:508–16.

32. Bae S-E, Corcoran BM, Watson ED. Immunohistochemical study of the distribution of adrenergic and peptidergic innervation in the equine uterus and the cervix. 2001;122:275-82

33. Krantz KE. INNERVATION OF THE HUMAN UTERUS*. Annals of the New York Academy of Sciences 1959;75:770–84.

34. Coupland RE. The distribution of cholinergic and other nerve fibres in the human uterus. Postgraduate Medical Journal 1969;45:78–9.

35. Newman TA, Bailey JL, Stocker LJ, Woo YL, Macklon NS, Cheong YC. Expression of neuronal markers in the endometrium of women with and those without endometriosis. Human Reproduction 2013;28:2502–10.

36. Mónica Brauer M, Smith PG. Estrogen and female reproductive tract innervation: Cellular and molecular mechanisms of autonomic neuroplasticity. Autonomic Neuroscience 2015;187:1–17.

37. Atwal G, du Plessis D, Armstrong G, Slade R, Quinn M. Uterine innervation after hysterectomy for chronic pelvic pain with, and without, endometriosis. Am J Obstet Gynecol 2005;193:1650–5.

Table 1: Summary table describing the neuronal finding and its site, putative physiologic function, and possible pathologic conditions that could lead to patient symptoms (pain, hyperalgesia)

Neuronal findings	Uterine sites	Putative physiologic function	Pathologic conditions
PS100: **All nerves** **Pan neuronal**	All layers: very abundant in the serosa +++ All portions: very abundant in the Cervix +++	- Uterine contractions (labour) - Uterine peristalsis (fertility) - Cervical ripening and opening (labor, fertility)	**Higher density** of nerves in myometrium and endometrium (especially in the functional layer) **Micro-neuroma formation** within the myometrium, hypertrophy of nerve termination
TH : **Autonomic sympathetic**	The most abundant type Present in all layers Present in all portions: especially in the cervix	- Endometrial glandular secretion - regulation of uterine blood flow	**Higher density** of nerves enabling **angiogenesis.** **Angiogenic and neurotrophic factors increase blood vessels and nerve density**
NPY : **Autonomic sympathetic**	Very abundant Present in all layers: especially myometrium and endometrium Present in all portions: less abundant in uterine body	- Endometrial glandular secretion - Regulation of uterine blood flow - Vasoconstrictor (boosts the adrenergic effect)	**Higher density** of nerves in the functional endometrium layer enabling **angiogenic and neurotrophic factors which increase blood vessel and nerve density** **Markers for sensory A delta and sensory C nerve fibers**
CGRP1 : **Sensory autonomic**	Present in all layers: especially myometrium and endometrium Present in all portions: most abundant in uterine body	- Vasodilatator - Smooth muscle cell relaxation - Inhibition of uterine contractions	**Higher density** of nerves contributing to the **inflammatory response** (vasodilation, plasma extravasation, infiltration by mast cells, neutrophils and immune cells). **Markers for sensory A delta and sensory C nerve fibers**
VIP : **Sensory** **Autonomic parasympathetic**	The least abundant type Present in all layers: less abundant in the endometrium All portions: equivalent abundance in the body and the cervix	- Vasodilatator - Smooth muscle cell relaxation - High uterine blood flow - Steroidogenesis - Ovulation, - Vaginal lubrification - Endometrial glandular secretion	**Higher density** of nerves in the functional endometrium layer contributing to the **inflammatory response** **Markers for sensory A delta and sensory C nerve fibers**
Nos: **Autonomic** **Parasympathetic** **Pro-erectile nerve bundles**	In the present study, only seen surrounding uterine artery	- Could play a role in maintaining uterine quiescence during pregnancy - Powerful inhibitor of platelet - Contributes to maternal systemic vasodilation during pregnancy, regulates uterine and fetoplacental blood flow - Degree of menstrual bleeding - Might participate in the initiation and control of menstrual bleeding	**NO deficiency contributes to the hypertensive disorder of pregnancy: preeclampsia**
Vacht: **Autonomic parasympathetic**	In the present study, only seen surrounding uterine artery Myometrium Cervix	- Associated with myometrial and vascular smooth muscle - Induces contraction of the myometrium	**Activation of sensory C nerve fibers** through nicotinic receptor neurons.

Figures Legends

Figure 1: Illustration of the use of immunofluorescence images to perform nerve quantification with the "HALO" software.

Section of the uterine body treated with triple SMA-TH-NPY labeling, with DAPI. Each fluorochrome can be "switched off" or "switched on" depending on what we want to visualize. This illustration shows the centripetal disposition of the innervation of the uterus.

A : SMA + TH + NPY + DAPI
B : SMA + TH + DAPI
C : SMA + NPY + DAPI
D : TH + NPY + DAPI
E: TH + NPY
F : endometrial contouring
G : myometrium contouring
H : contouring of the serosa
I : contouring of the whole uterus

Figure 2: Organization of nerve fibers within the myometrium on a cross-section at the uterine isthmus.

Nerve fibers are preferably perivascular (black arrowheads), or they travel between muscle cells parallel to the axis of the muscular fibers (black arrows).

a: arterioles; OA : ombilical artery ; U : ureter ; v: veins

Figure 3: Computer Assisted Anatomical Dissection (CAAD) of the uterine innervation shown in posterior and superior views.

We focused our reconstruction on the lower part of the uterus, from the lower part of the uterine body to the tip of the cervix. It clearly illustrates the centripetal organisation of the uterine nerve fibers, with fibers ascending to the uterine body, and descending to the cervix.

ICO = internal cervical orifice; IHP = inferior hypogastric plexus; U = ureter ; UA = uterine artery

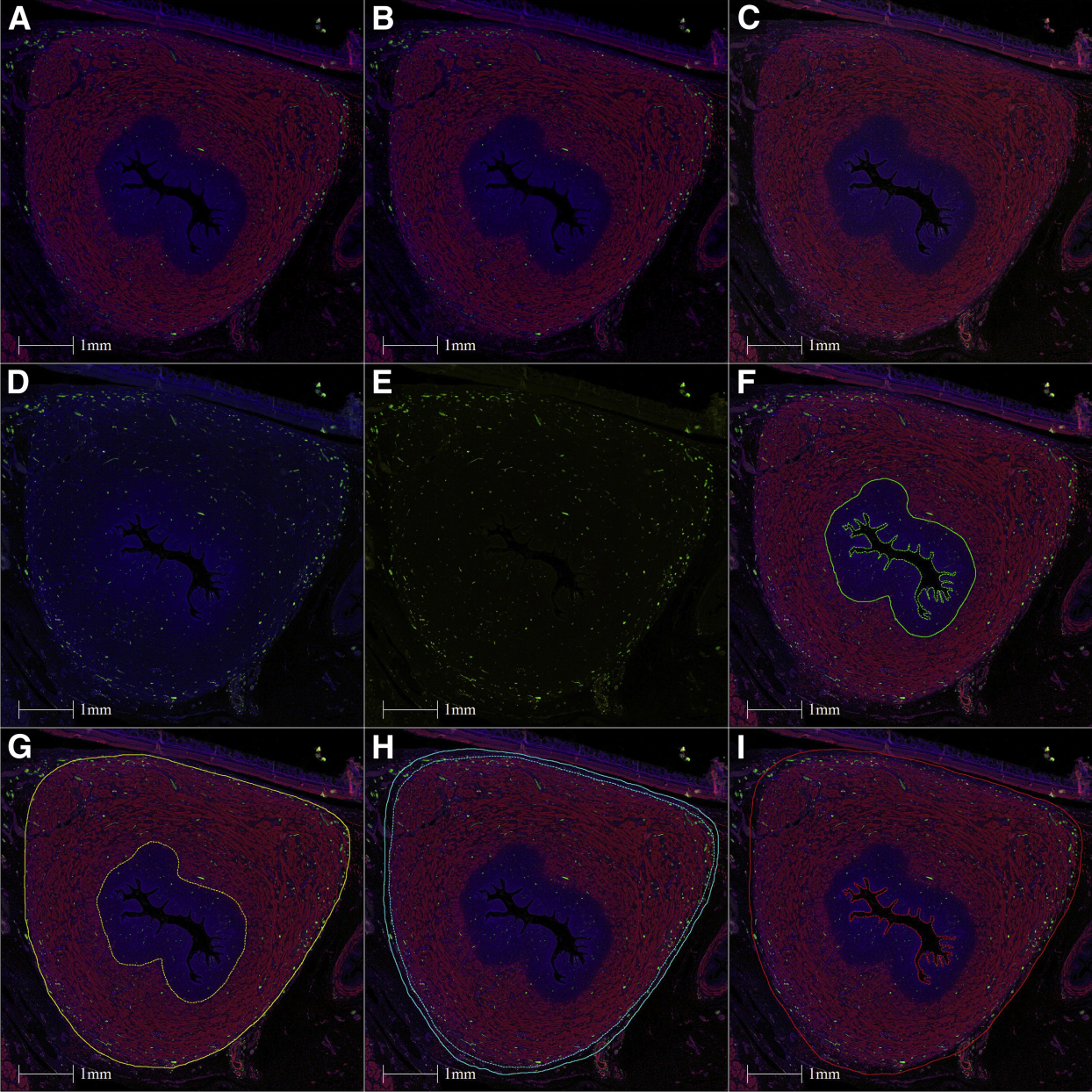
A
1mm
B
1mm
C
1mm
D
1mm
E
1mm
F
1mm
G
1mm
H
1mm
I
1mm

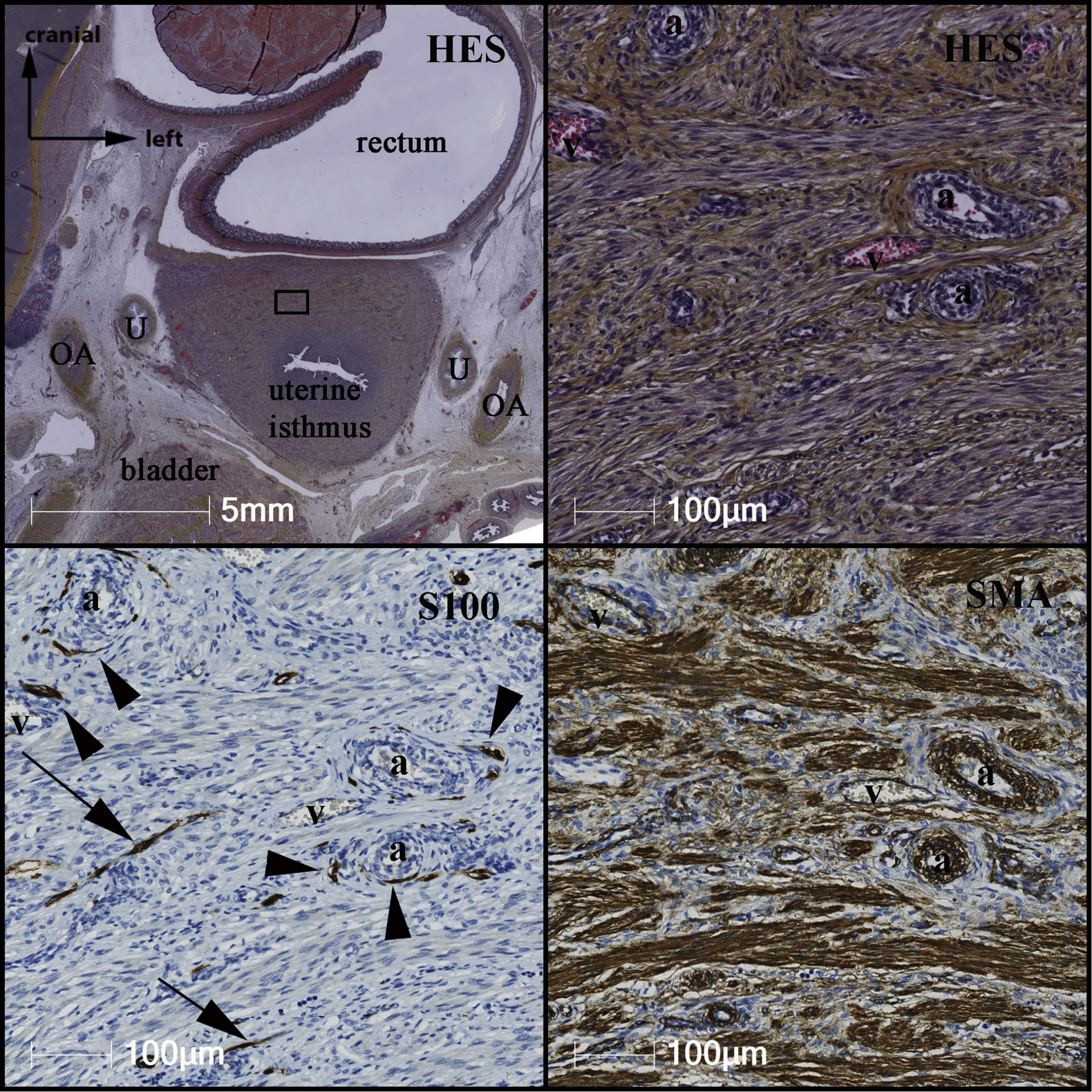
cranial
left
HES
rectum
U
OA
uterine
isthmus
U
OA
bladder
5mm
a
HES
v
a
v
a
100µm
a
S100
v
a
v
a
100µm
v
SMA
a
v
a
100µm

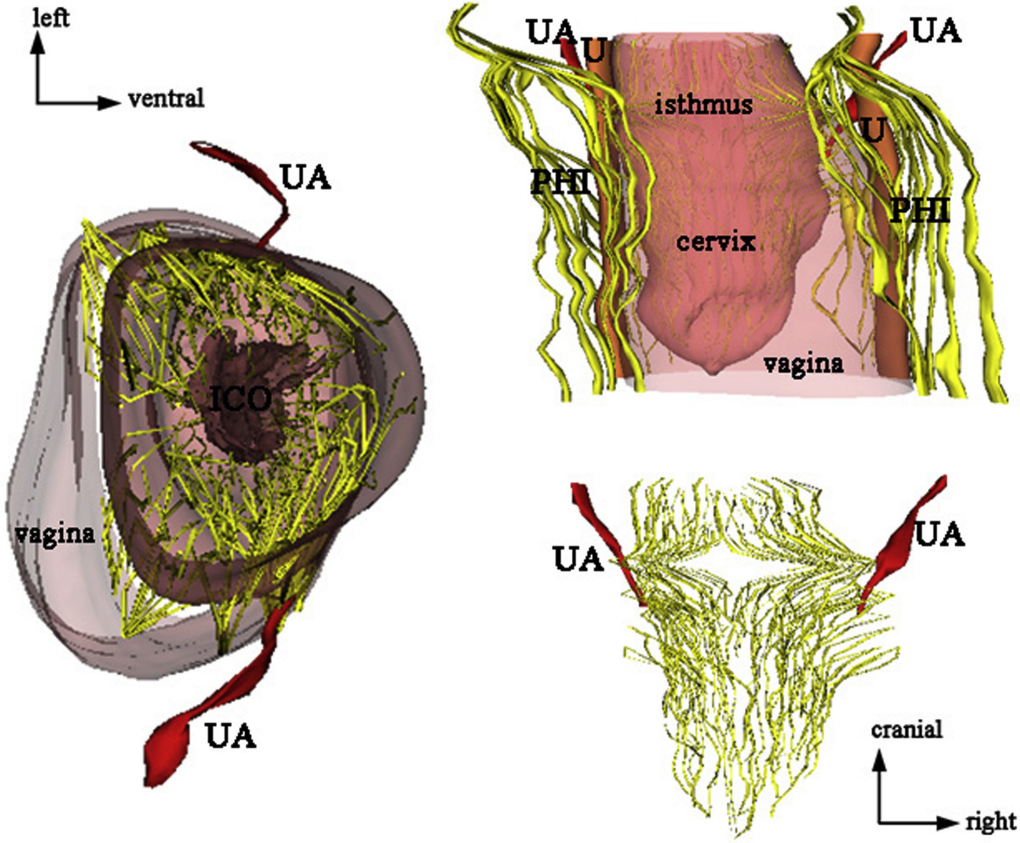
left
ventral
UA
ICO
vagina
UA
UA
U
isthmus
U
UA
PHI
PHI
cervix
vagina
UA
UA
cranial
right

Supplemental Materials

Supplemental Table 1: Primary antibodies

Antibody	Lab	Source	Reference	Clone	Batch number	Isotype	Conditioning	Dilution IHC	Dilution IF	Control tissue
PS100	Biocare Medical	Ms	cm128C	15E2E2	50815	IgG2a	+4°C	1/50	1/500	Human sacral plexus
PMP22	Abcam	Rb	ab15506	Poly	GR3204713-1	IgG	-20°C	1/200	1/1000	Human brain
NNOS	Cayman	Rb	160870	poly	05110674-1	IgG	-20°C	1/400	1/2000	Human brain
CGRP1	Novusbio	Ms	NBP1-05164	5	M0314	IgG1-K	+4°C	1/50	1/100	Human pancreas
TH	Abcam	Rb	ab112	Poly	GR286793-17	IgG	-20°C	1/750	1/1000	Human brain and adrenals
SMA	Dako	Ms	M0851	1A4	59322	IgG2	+4°C	1/300	1/3000	Human colon
Oxytocin	Novusbio	Rb	NBP2-68928	Poly	R103765	IgG	-20°C	1/50	1/50	Human endometrium and ovaries
NPY	Novusbio	Rb	NBP2-38804	Poly	R77673	IgG	-20°C	1/50	1/100	Human brain
VIP	Novusbio	Ms	NBP1-05163	2	L1217	IgG1-K	+4°C	1/50	1/100	Human brain
RLN2	Abcam	Rb	ab183505	EPR14205	GR1533833-8	IgG	-20°C	1/2000	1/6000	Human brain and placenta
VACHT	invitrogen	Rb	PA5-85782	Poly	VF3005506C	IgG	-20°c	1/1000	1/3000	Rat spinal cord

Ms = mouse ; Rb = rabbit ; poly = polyclonal ; IHC = immuno-histochemistry ; IF = immunofluorescence

Supplemental Figure/video 1: Animation of a 3D reconstruction of uterine micro-innervation model focusing on the lower part of the fetal human uterus.

Nerve fibers penetrate the uterus through the lateral edges of the uterine isthmus. They then follow a centripetal path from the periphery (serosa) to the center (endometrium) with ascending fibers towards the uterine body and descending fibers towards the cervix.

Supplemental Figure 2: Structure and innervation of the endometrium.

Cross sections of the uterine body, treated with HES (A), anti-SMA (B), and anti-S100 (C).

The black arrowheads refer to nerve fibers in the functional layer of the endometrium.

ICO: internal cervical orifice

Supplemental Figure 3: Endometrial innervation at the uterine isthmus.

The white arrowheads indicate the characteristic markings of the presence of nerve fibers, with a reticular organization.

The red ellipses indicate areas of markings characteristic of a “background noise” in immunofluorescence.

The anti-S100, TH, NPY, CGRP1 and VIP immunostaining is positive, and the anti-oxytocin marking is presented as an example of negative marking with "background noise". The other labels not shown were all negative.

Supplemental Figure 4: Graph representing the nerve density in each portion and layer of the uterus (in % of the studied surface) calculated with the "HALO" software.

The density of nerve fibers is the highest in the supra-vaginal portion of the cervix, and higher in the serosa in periphery. Nerve fibers are rare but present in the endometrium.

Supplemental Figure 5: Specificity of nerve fibers in the three portions of the uterus: body (A), supra-vaginal cervix (B), and intra-vaginal cervix (C)

Only positive markings are presented here (white arrowheads).

Nerve fibers TH+, NPY+, CGRP1+ and VIP+ are found in all three layers of the cervix and three portions of the uterus.

OA: ombilical artery; U: ureter; vcds: vaginal cul-de-sac

Supplemental Figure 6: Detailed specificity of nerve fibers in the intravaginal cervix.

Only positive markings are presented here (white arrowheads and black arrowshead).

OA: ombilical artery; U: ureter; vcds: vaginal cul-de-sac

Supplemental Figure 7: Detailed specificity of nerve fibers in the body of the uterus.

Only positive markings are presented here (white arrowheads and black arrowshead).

UA: uterine artery; U: ureter;

Supplemental Figure 8: Detailed specificity of nerve fibers in the supravaginal cervix.

Only positive markings are presented here (white arrowheads and black arrowshead).

OA: ombilical artery; U: ureter;

Supplemental Figure 9: Innervation of the uterine artery observed by immunohistochemistry.

Nerve fibers originate in the IHP and follow the course of the uterine artery in front of the ureter

Black arrowheads mark positive stainings. Autonomous innervation TH+, VACHT+, and weakly nNOS+ is found, but also sensitive innervation CGRP1+ and NPY+ on direct contact with the media.

All nerve fibres are VIP-, RLN2-, Oxytocin- and PMP22-.

IHP = inferior hypogastric plexus

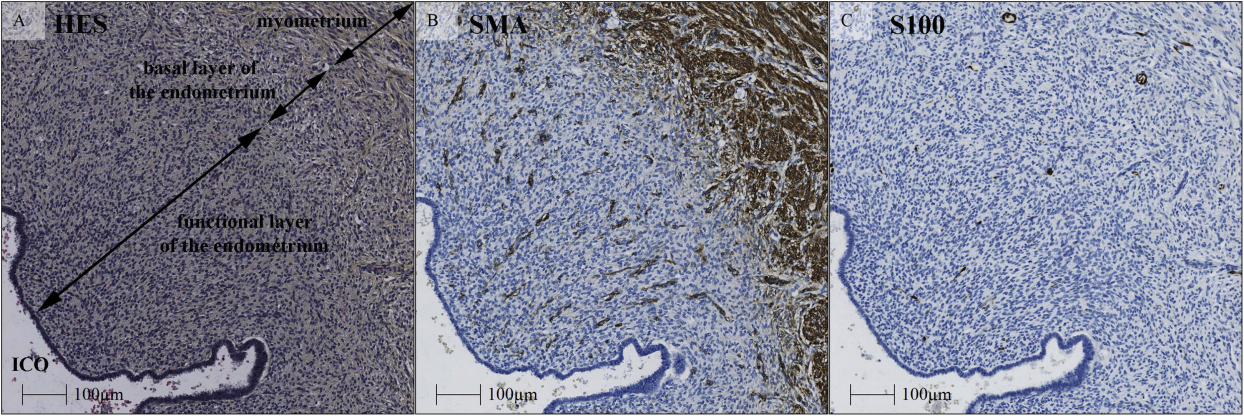
A
HES
myometrium
basal layer of
the endometrium
functional layer
of the endometrium
ICO
100µm
B
SMA
100µm
C
S100
100µm

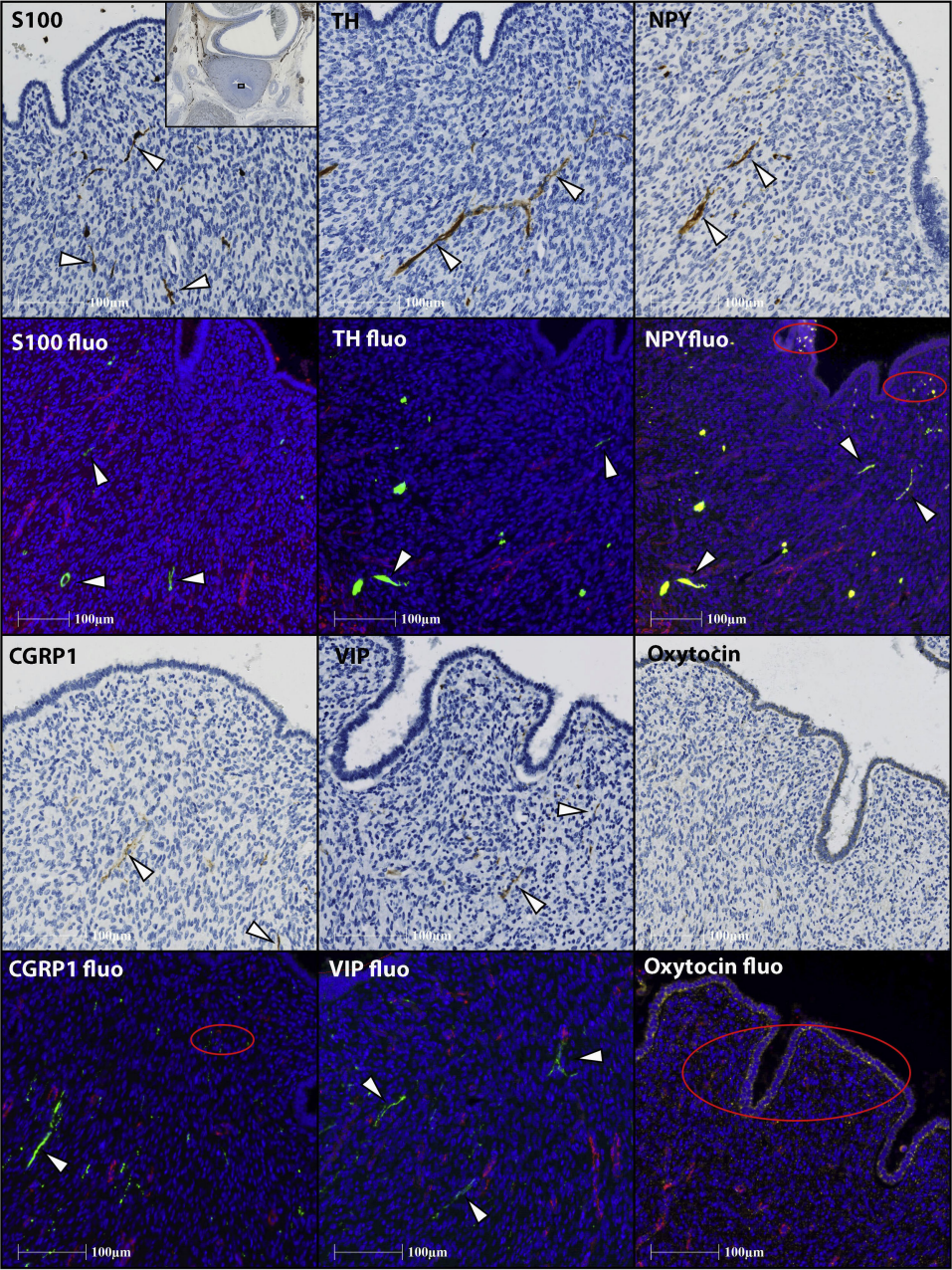
S100
TH
NPY
S100 fluo
TH fluo
NPYfluo
CGRP1
VIP
Oxytocin
CGRP1 fluo
VIP fluo
Oxytocin fluo
100µm

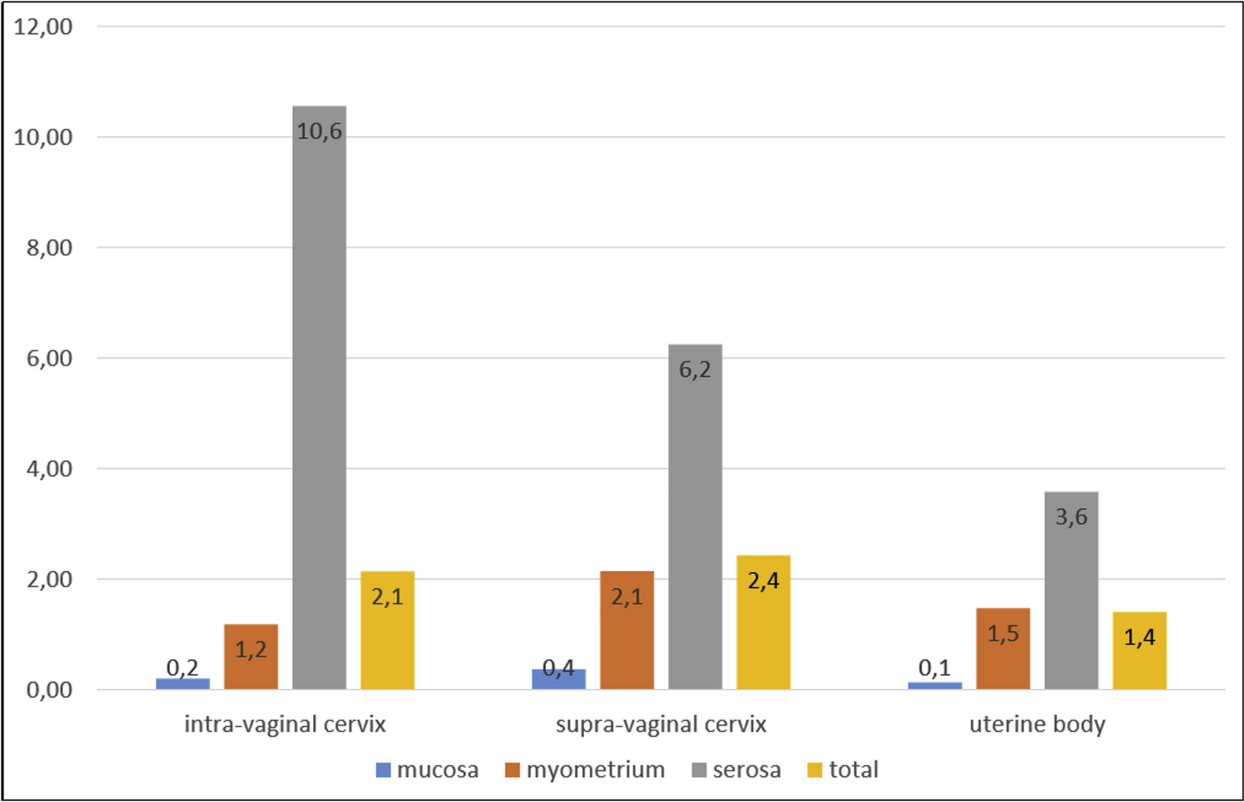
12,00
10,00
8,00
6,00
4,00
2,00
0,00
0,2
1,2
10,6
2,1
0,4
2,1
6,2
2,4
0,1
1,5
3,6
1,4
intra-vaginal cervix
supra-vaginal cervix
uterine body
mucosa
myometrium
serosa
total

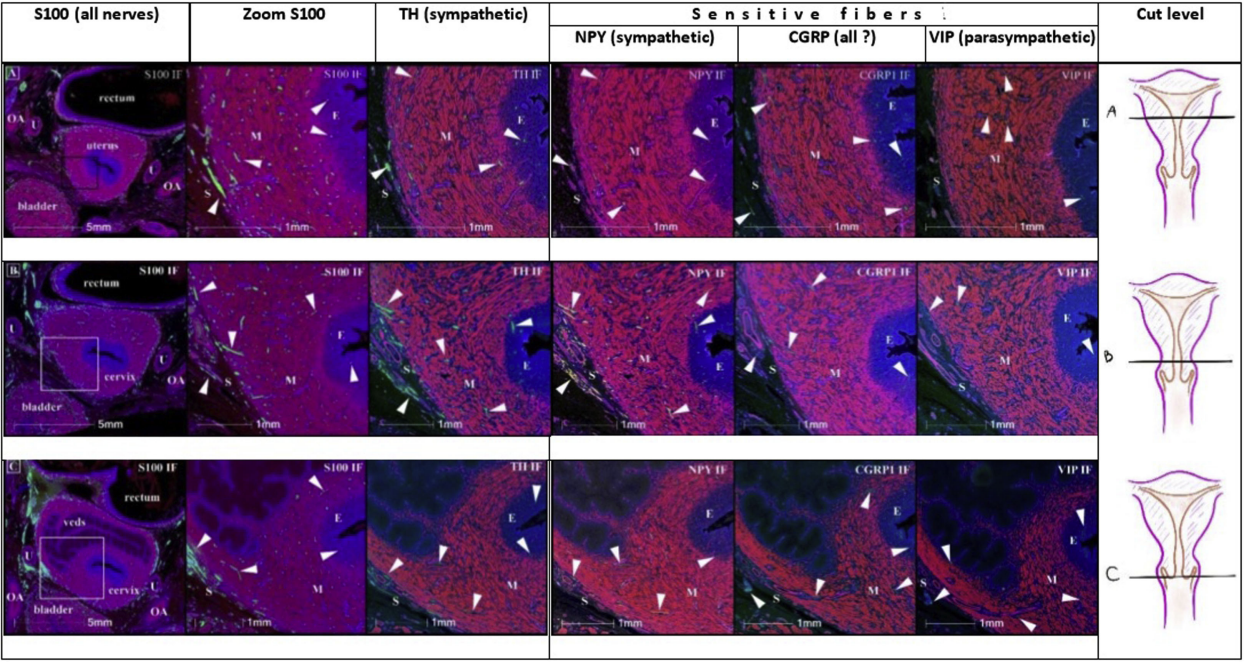
S100 (all nerves)
Zoom S100
TH (sympathetic)
Sensitive fibers :
NPY (sympathetic)
CGRP (all ?)
VIP (parasympathetic)
Cut level
A
S100 IF
rectum
uterus
bladder
OA
U
M
E
S
5mm
1mm
TH IF
NPY IF
CGRP1 IF
VIP IF
B
cervix
C
veds

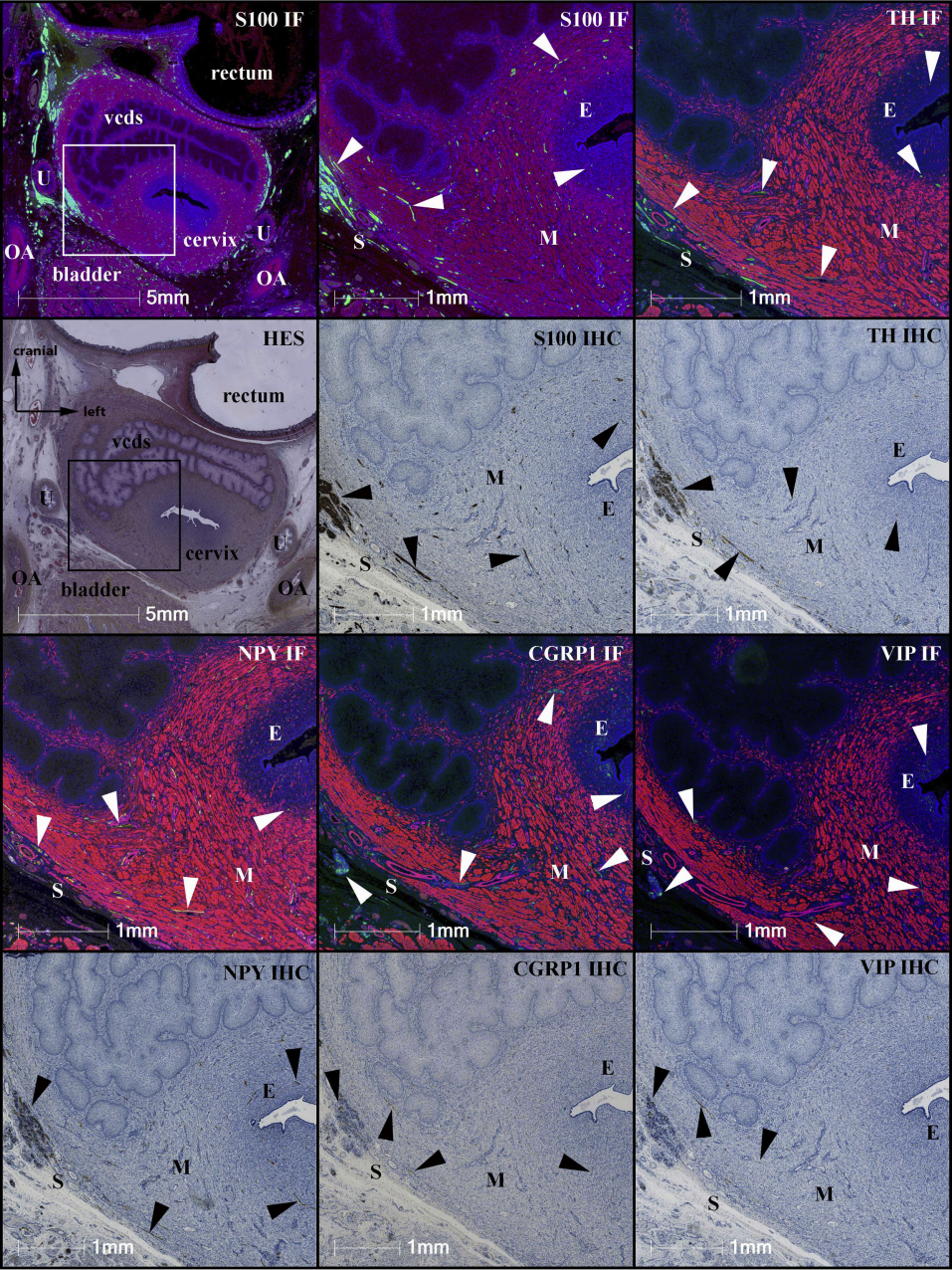
S100 IF
rectum
vcds
U
OA
cervix
U
bladder
OA
5mm
S100 IF
E
S
M
1mm
TH IF
E
M
S
1mm
HES
cranial
left
rectum
vcds
U
cervix
U
OA
bladder
OA
5mm
S100 IHC
M
E
S
1mm
TH IHC
E
S
M
1mm
NPY IF
E
S
M
1mm
CGRP1 IF
E
M
S
1mm
VIP IF
E
S
M
1mm
NPY IHC
E
S
M
1mm
CGRP1 IHC
E
S
M
1mm
VIP IHC
E
S
M
1mm

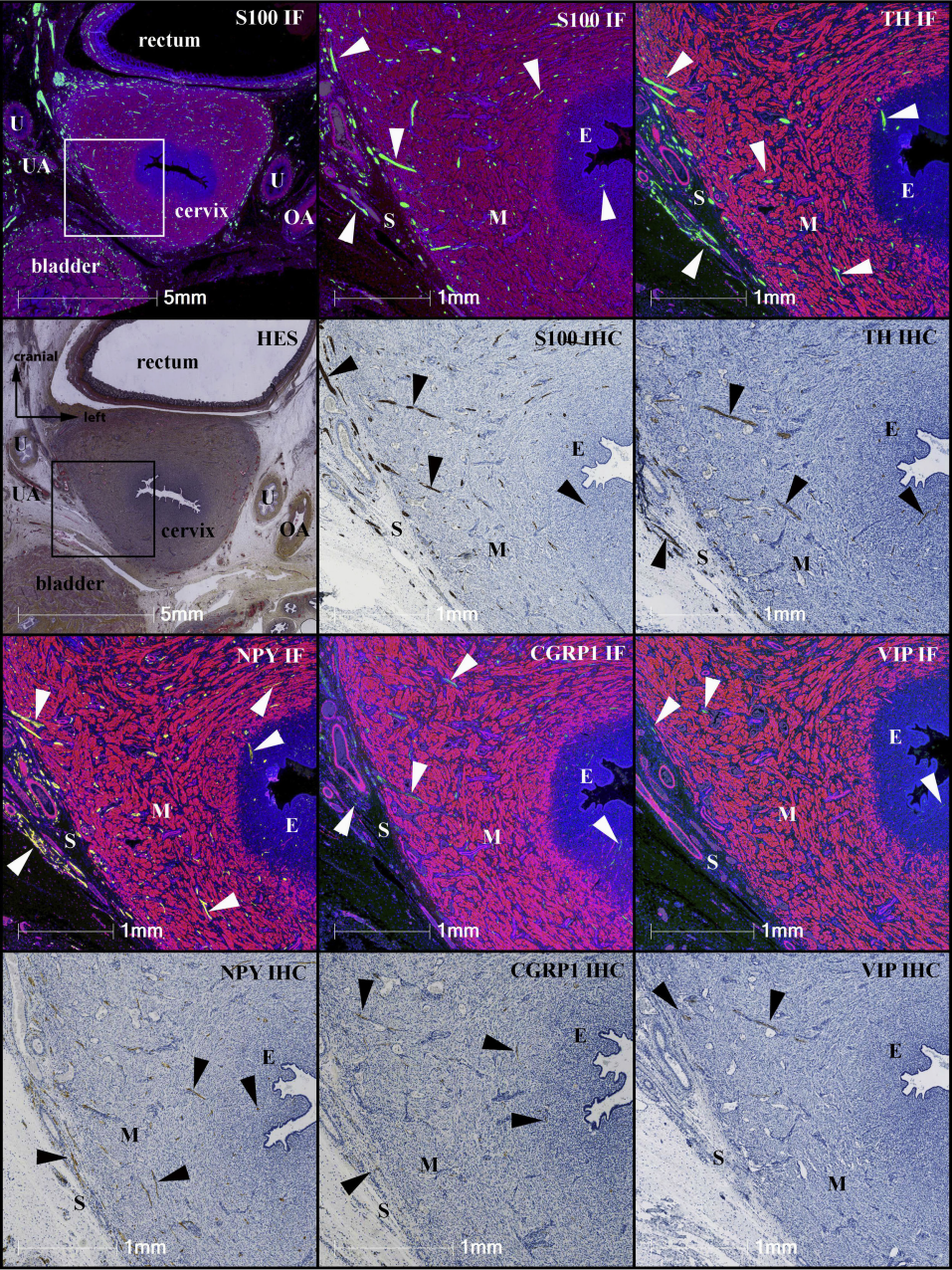
S100 IF
rectum
U
UA
U
OA
cervix
bladder
5mm
S100 IF
E
S
M
1mm
TH IF
S
E
M
1mm
HES
cranial
left
rectum
U
UA
U
OA
cervix
bladder
5mm
S100 IHC
E
S
M
1mm
TH IHC
E
S
M
1mm
NPY IF
M
E
S
1mm
CGRP1 IF
E
S
M
1mm
VIP IF
E
M
S
1mm
NPY IHC
E
M
S
1mm
CGRP1 IHC
E
M
S
1mm
VIP IHC
E
S
M
1mm

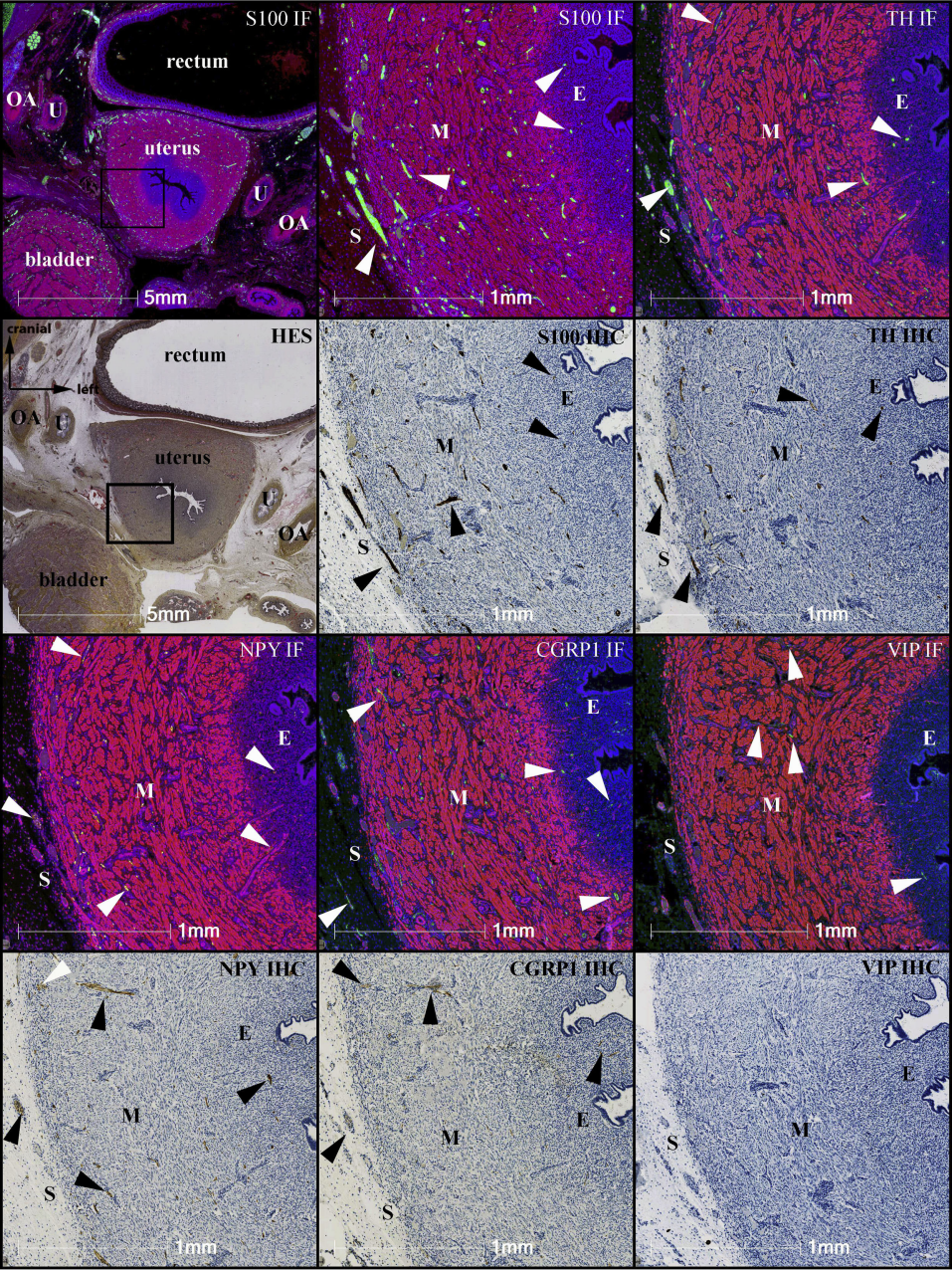
S100 IF
rectum
OA
U
uterus
U
OA
bladder
5mm
S100 IF
E
M
S
1mm
TH IF
E
M
S
1mm
cranial
left
HES
rectum
OA
U
uterus
U
OA
bladder
5mm
S100 IHC
E
M
S
1mm
TH IHC
E
M
S
1mm
NPY IF
E
M
S
1mm
CGRP1 IF
E
M
S
1mm
VIP IF
E
M
S
1mm
NPY IHC
E
M
S
1mm
CGRP1 IHC
E
M
S
1mm
VIP IHC
E
M
S
1mm

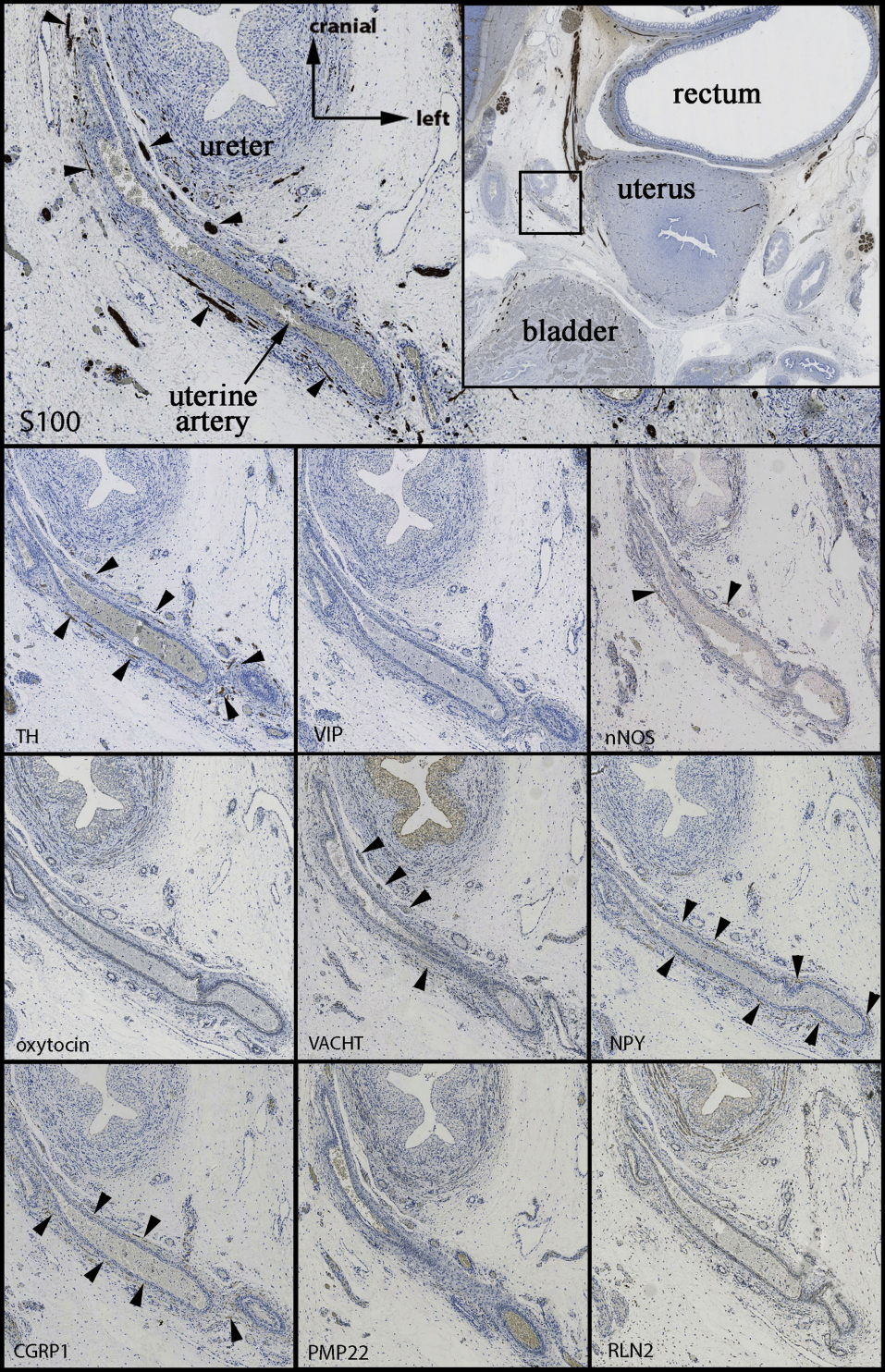
cranial
left
ureter
uterine artery
S100
rectum
uterus
bladder
TH
VIP
nNOS
oxytocin
VACHT
NPY
CGRP1
PMP22
RLN2